Pergamon

Int. J. Heat Mass Transfer. Vol. 41, No. 11, pp. 1613–1619, 1998

Printed in Great Britain
0017-9310/98 $19.00+0.00

PII: S0017-9310(97)00244-5

Finite element analysis of mixed convection over in-line tube bundles

Y. T. KRISHNE GOWDA
P.E.S. College of Engineering, Mandya 571 401, India

P. A. ASWATHA NARAYANA
Department of Applied Mechanics

and

K. N. SEETHARAMU
Department of Mechanical Engineering, Indian Institute of Technology, Madras 600 036, India

(*Received* 27 *October* 1995 *and in final form* 16 *July* 1997)

Abstract—Heat transfer and fluid flow over in-line bundles of cylinders have been numerically simulated. Flow is assumed as incompressible, two-dimensional and laminar. Analysis has been carried out for Reynolds numbers of 50, 100, 150 and pitch to diameter ratios (PDR) of 1.5 and 2.0 with a Prandtl number of 0.71. The effect of Richardson number ($Ri = Gr/Re^2$) on the flow and heat transfer has been investigated for $Ri = -1.0, -0.5, 0.0, +0.5$ and $+1.0$. Streamlines, temperature contours, average Nusselt numbers, average friction coefficients and pressure distribution around the cylinders are presented. It is observed that there is a considerable effect of buoyancy over tube bundles.

1. INTRODUCTION

The problem of mixed convective heat transfer from tube bundles has received considerable attention in view of its fundamental nature and practical applications in heat exchangers, electronic equipment cooling and solar thermal extraction systems. As a result, extensive experimental and theoretical works have been conducted on heat transfer from a single cylinder in the past [1–4]. Ho *et al.* [5] have made a numerical study on the buoyancy-aided steady convection heat transfer from a horizontal cylinder situated in a vertical adiabatic duct. The phenomenon of vortex shedding from a heated/cooled circular cylinder has been investigated in the mixed convection regimes by Keun-shik Chang and Jong-youb Sa [6].

Forced convection over tube bundles has been studied widely and a few are summarized below. Experimental data on flow and heat transfer characteristics for various arrangements of in-line bundles of cylinders have been presented by Zukauskas *et al.* [7]. The rapid development of computers has resulted in the use of numerical simulation for the solution of heat and momentum transfer problems in tubular heat exchangers. Ishihara and Bell [8] obtained the friction coefficients of tube bundles upto a Reynolds number of 100. Fujii *et al.* [9] have studied a five row deep tube bank with pitch to diameter ratio of 1.5 for Reynolds numbers upto 300. The heat flux between the third and fourth row in a five row bundle of cylinders will approximately represent the heat flux between two adjacent inner rows of an infinite bundle of cylinders. Dhaubhadel *et al.* [10] have studied flow across in-line bundles of cylinders with pitch to diameter ratios of 1.25, 1.5 and 1.8. Reynolds number range studied is from 100 to 600 and Prandtl number is taken as 0.7. Yeon Chang *et al.* [11] developed a numerical scheme to predict the heat transfer and pressure drop coefficients for flow past rigid tube bundles for pitch to diameter ratios of 1.5 and 2.0 and Reynolds number upto 1000.

At these low Reynolds numbers, buoyancy has a significant influence on the flow over tube bundles. In the above cited literature, the authors have neglected the effect of buoyancy on the flow and heat transfer. Also, the problem of mixed convection over tube bundle has not been reported so far.

In the present study, a finite element approach has been employed to solve the two-dimensional Navier–Stokes equations along with energy equation, for laminar flow of an incompressible fluid past an in-line bundle of cylinders having pitch to diameter ratios of 1.5 and 2.0 with Reynolds number of 50, 100 and 150. Richardson numbers of $-1.0, -0.5, 0.0, 0.5$ and 1.0 are considered for the study.

Solution procedure

The solution algorithm employed in the present study is an Eulerian velocity correction method [12, 13]. In this method, the solution is advanced in three steps within each time step. The three steps involved

NOMENCLATURE

C_p	specific heat
D	diameter of the cylinder
f_{vs}	vortex shedding frequency
g	gravitational acceleration
Gr	Grashof number $(\beta g(T_w - T_{in})D^3/\nu^2)$
K	thermal conductivity
Nu	Nusselt number (hD/K)
P	non-dimensional pressure $(p/\rho U_{av}^2)$
Pe	Peclet number $(Re\ Pr)$
Pr	Prandtl number $(\mu C_p/K)$
Re	Reynolds number $(U_{av}\ D/\nu)$
Ri	Richardson number (Gr/Re^2)
St	Strouhal number $(f_{vs}\ D/U)$
T	temperature
T_{in}	inlet temperature
T_w	cylinder surface temperature
U_{av}	average velocity at minimum cross sectional area
U	non-dimensional axial velocity (u/U_{av})
V	non-dimensional normal velocity (v/U_{av})
X	non-dimensional axial coordinates (x/D)
Y	non-dimensional normal coordinates (y/D).

Greek symbols

θ	non-dimensional temperature $(T-T_{in})/(T_w-T_{in})$
ν	dynamic viscosity
ρ	density
τ	non-dimensional time (D/U_{av}).

Subscripts

av	average
in	free-stream condition
w	wall.

are the calculation of pseudo velocities, evaluation of pressure from Poisson equation and the correction of pseudo velocities to obtain correct velocities at the next time step. Since the velocities are dependent on temperature, the momentum and energy equations are solved as coupled equations.

Finite element discretization and problem statement

The finite element spatial discretization is performed using linear triangular elements. Galerkin weighted residual technique is used to formulate the problem. The details of the shape (interpolation) functions used for the variables are available in Segerlind [14].

In order to validate the code, flow over a single cylinder for $Re = 100$ and $Pr = 0.7$ is investigated for the case of $Ri = 0.0$. The average Nusselt numbers and Strouhal number are found to be in good agreement with the earlier investigations as shown in Table 1.

2. MATHEMATICAL MODEL

For two-dimensional flow of an incompressible fluid with negligible viscous dissipation, the non-dimensional form of Navier–Stokes equations and energy equation can be written as

$$\text{Continuity:}\quad \frac{\partial U}{\partial X}+\frac{\partial V}{\partial Y}=0 \tag{1}$$

$$\text{Momentum:}\quad \frac{\partial U}{\partial \tau}+U\frac{\partial U}{\partial X}+V\frac{\partial U}{\partial Y} = -\frac{\partial P}{\partial X}+\frac{1}{Re}\left(\frac{\partial^2 U}{\partial X^2}+\frac{\partial^2 U}{\partial Y^2}\right)+Ri\theta \tag{2}$$

$$\frac{\partial V}{\partial \tau}+U\frac{\partial V}{\partial X}+V\frac{\partial V}{\partial Y} = -\frac{\partial P}{\partial Y}+\frac{1}{Re}\left(\frac{\partial^2 V}{\partial X^2}+\frac{\partial^2 V}{\partial Y^2}\right) \tag{3}$$

Table 1.

Classification	Contributors	*Nu*	*St*
Experimental	Eckert and Soehngen (1952)	5.23	
	Tritton (1959)		0.157
	Berger (1965)		0.155
Numerical	Jordan and Fromm (1972)		0.16
	Jain and Goel (1976)	5.63	0.15
	Keun-Shik Chang *et al.* (1990)	5.23	0.155
	Present	5.39	0.151

$$\text{Energy}: \quad \frac{\partial\theta}{\partial\tau}+U\frac{\partial\theta}{\partial X}+V\frac{\partial\theta}{\partial Y}=\frac{1}{Pe}\left(\frac{\partial^2\theta}{\partial X^2}+\frac{\partial^2\theta}{\partial Y^2}\right) \tag{4}$$

In the above equations velocities are made dimensionless using the average velocity U_{av} at the minimum cross sectional area and the coordinates by using the tube diameter D. Reynolds number Re is based on the minimum flow area and U_{av}.

Boundary and initial conditions

The boundary and initial conditions for the variables are as follows.

Boundary conditions:

Cylinder surface: No slip ($U = V = 0.0$) and $\theta = 1.0$
Axis of symmetry: $V = 0.0$
Inlet: uniform flow and $\theta = 0.0$
Exit: pressure boundary condition, $P = 0$.

Initial conditions:

At $\tau = 0$: $U = 0$, $V = 0$, $P = 0$ and $\theta = 0.0$.

The flow geometry for a five row deep tube bundle is shown in Fig. 1. Owing to symmetry, the region between the broken lines is used as the computational domain.

Grid independence test

The following three types of mesh are considered for the grid sensitivity analysis.

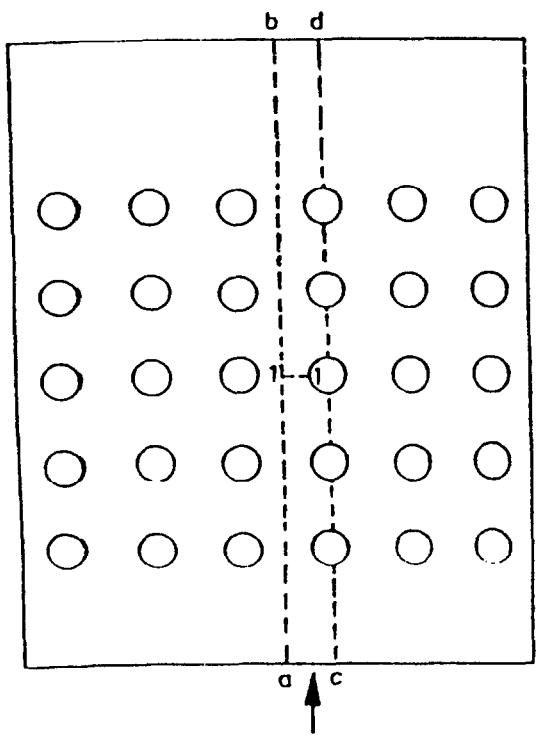

Fig. 1. Flow geometry.

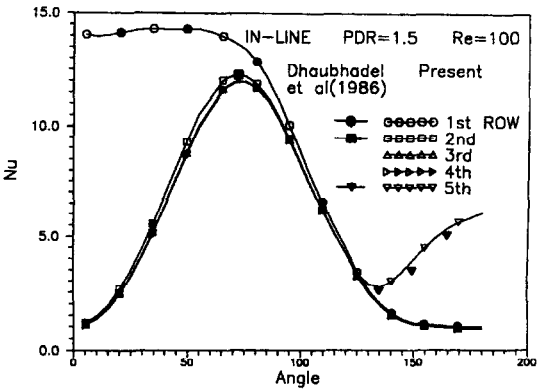

Fig. 2. Comparison of local Nusselt numbers.

(A) 1727 nodes; 3072 elements
(B) 2539 nodes; 4608 elements
(C) 2945 nodes; 5376 elements

In the present computations a grid with 2539 nodes and 4608 elements has been found to be sufficient for the analysis. The computational results show a maximum difference of about 1.5% in the local and average Nusselt numbers between grids of type B and C. The B type mesh has been chosen since the results predicted from this mesh also agree well with the available experimental and numerical results for the forced convection problem over in-line tube bundles. A typical computed Nusselt number distribution in comparison with results obtained by Dhaubhadel *et al.* [10] is shown in Fig. 2.

A steady state condition is assumed to have been reached, if the changes in velocity, pressure and temperature anywhere within the domain after two successive iterations are less than 0.00001.

3. RESULTS AND DISCUSSIONS

The main purpose of this paper is to study the effect of buoyancy on pressure drop and heat transfer. The flow geometry for a five row deep in-line bundle of cylinders is shown in Fig. 1. The boundary conditions are given as above.

Streamlines

Figure 3 shows streamlines for pitch to diameter ratio of 2.0, Reynolds number of 100 and for different Richardson numbers.

Forced convection: It is observed that for a particular Reynolds number, separation and reattachment points are the same for all cylinders except for the last row. The recirculation region between the cylinders can be clearly seen in Fig. 3. The strength of the recirculation between cylinders is found to increase with increase in Reynolds number. The recirculating flow region on the leeward side of the cylinder becomes larger and thus the separation point moves

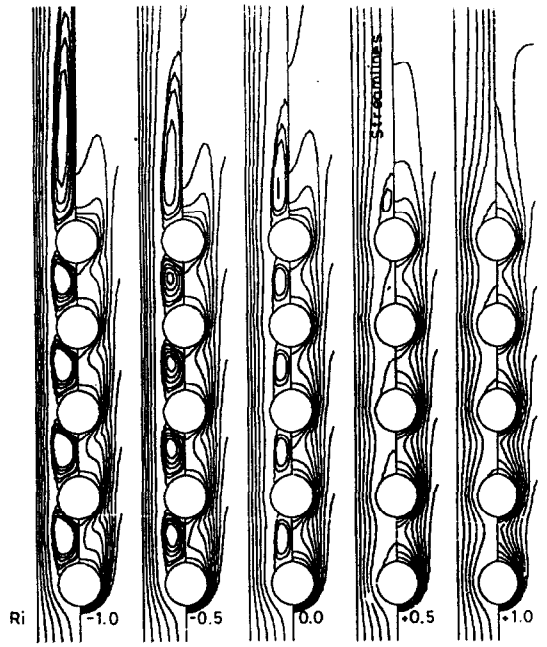

Fig. 3. Streamlines and isotherms.

away from the rear stagnation point. The angle of separation/reattachment (measured from the front stagnation point) decrease/increase with increase in Reynolds number which is due to increase in the strength of recirculation. The length of recirculatory region increases behind the fifth row of cylinders with increase in Reynolds number. Similar trend is seen for pitch to diameter ratio of 2.

Buoyancy aided convection: The effect of buoyancy aiding force on the flow pattern is also examined in Fig. 3. The cases of $Ri = 0.5$ and $Ri = 1.0$ refer to the buoyancy aided convective situation. It can be noticed, that Reynolds number, PDR and the position of the cylinder in the bank have a marked influence on the size of the recirculatory region. When compared with the case of pure forced convection ($Ri = 0.0$), one can see that the aiding buoyancy force diminishes the wake region on the rear side of the cylinders and thus the separation point is shifted downstream. Above a certain threshold value of Ri, no separation occurs. As Ri increases from 0.5 to 1.0, recirculatory regions either vanish or they become very small in size. In general, the influence of assisting buoyancy force on the flow pattern for PDR = 2.0 is more than that for PDR = 1.5.

Buoyancy opposed convection: $Ri = -0.5$ and -1.0 correspond to the case of buoyancy opposed convection. The size of the recirculatory zone is again dependent on PDR, Reynolds number and the position of the cylinder in the bank. Compared to the case of pure forced convection ($Ri = 0$), one can see that the opposing buoyancy force has increased the strength of the recirculatory region between the cylinders. It can be seen that the strength of the recirculatory eddy between the cylinders is decreasing with the increasing number of rows. The flow behind the fifth row results in a much bigger recirculatory zone with increasing Re. It can also be seen that Ri affects the size of the recirculatory region between the cylinders. Since the flow is opposing and the size of the recirculatory zone increases and the separation points move towards the leeward side. On the contrary, the reattachment points move towards the aft. This trend can be noticed for both the pitch to diameter ratios considered.

Isotherms

The isotherms shown in Fig. 3 are crowded over the entire front half of the first row indicating a high radial heat flux. This is understandable since the thermal boundary layer growth begins from the first row. Over the other rows, low velocity recirculating flow interacts with part of the front half. It is also seen from the plots that there is crowding of isotherms only over those portions where the flow has not separated. The isotherms are qualitatively similar for different Richardson numbers. With the increase in PDR to 2.0, more crowding of isotherms can be seen in all the rows of cylinders when compared to PDR = 1.5. Similar trends can be seen even with increase in Reynolds number.

Skin friction coefficient

The distribution of local friction coefficient is defined by

$$C_f(\theta) = \frac{\tau}{\frac{1}{2}\rho U_i^2} \tag{5}$$

The average friction coefficient is given by

$$\bar{C}_f = \frac{1}{\pi}\int_0^{\pi} C_f(\theta)\,d\theta \tag{6}$$

Figure 4(a) and (b) show the variation of average friction coefficient with Richardson number for pitch to diameter ratio of 1.5 and 2.0, respectively. Friction coefficient increases with increase in Richardson number for all the Reynolds numbers considered. In the opposing case, it is found that the average friction coefficient increasing as we go from the 2nd row to 5th row, whereas for the aiding case the trend is reversed. Similar behaviour is seen with increase in Reynolds number. Also it can be observed from the plots that, the difference in the values of average friction coefficients between the cylinders decreases with Reynolds number as well as PDR.

Nusselt number

Local Nusselt number is defined by

$$Nu(\theta) = \frac{T_w - T_{in}}{T_w - T_b}\left.\frac{\partial\theta}{\partial r}\right|_{r=R} \tag{7}$$

The average Nusselt number is given by

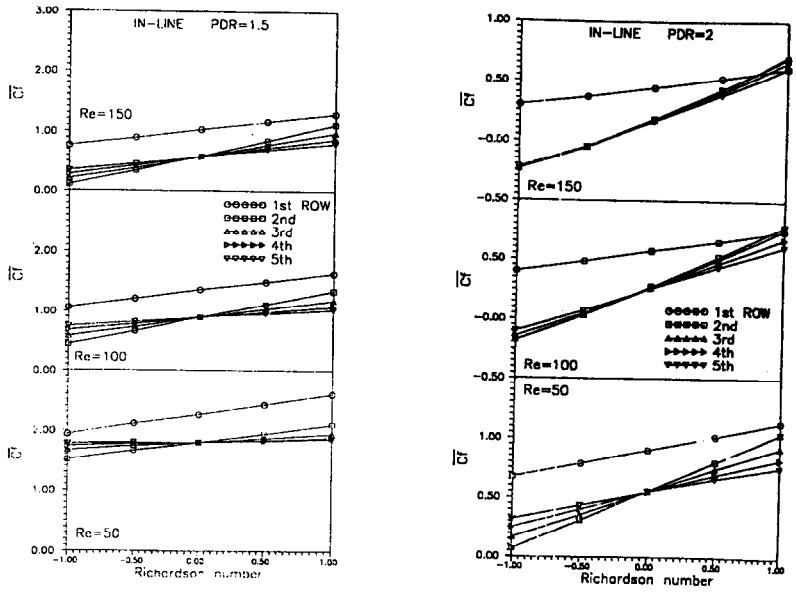

(a) In-line tube bank: PDR=1.5

(b) In-line tube bank: PDR=2.0

Fig. 4. (a) Variation of average friction coefficients. PDR = 1.5. (b) Variation of average friction coefficients. PDR = 2.0.

$$\bar{Nu} = \frac{1}{\pi}\int_0^{\pi} Nu(\theta)\,\mathrm{d}\theta \tag{8}$$

Figure 5(a) and (b) show the variation of average Nusselt number with Richardson number, for pitch to diameter ratio of 1.5 and 2.0, respectively. Average Nusselt number increases rapidly with increase in Richardson number over the first row of cylinders. Over rest of the rows, there is a marginal change with increase in *Ri*. Also it is observed from the plots that the average Nusselt number over the fifth row of cylinders is more than that of the rest of the cylinders. The difference in the average values of the Nusselt number between the last row and rest of the row of cylinders is found to increase with the increase in Reynolds number, with an exception for first row of cylinders. In the case of PDR = 2.0 the variation of average Nusselt number with *Ri* from second row onwards is only marginal. Also the average Nusselt number over all the rows of cylinders is lower than that of PDR = 1.5. Similar trend has been observed by Dhaubhadel *et al.* for $Ri = 0.0$. Figure 5(c) also shows the effect of buoyancy on the averaged Nusselt number for different pitch to diameter ratios.

Pressure coefficient

The pressure coefficient is defined by

$$C_p = \frac{P - P_i}{\frac{1}{2}\rho U_i^2} \tag{9}$$

Figure 6(a) and (b) show the pressure distribution along CD of the computational domain for PDR = 1.5 and 2.0, respectively. The pressure distribution over the first row for $Ri = 0.0$ is almost identical with a single cylinder case. From the second row onwards, the pressure drop from one row to the next is almost the same which is consistent with the flow field described earlier. Till the boundary layer separation on the first row of cylinders, the pressure coefficient is independent of *Ri*. The pressure drop is increased with a decrease in *Ri* and is maximum at $Ri = -1.0$. This is because the flow is opposed by the buoyancy. As *Re* is increased from 50 to 150 the pressure drop decreases and this is due to the fact that the inertial forces dominate over the buoyancy forces. Pressure recovery is observed due to the buoyancy force which is aiding the flow. This pressure recovery increases with the increase in Richardson number. For higher PDR, the pressure recovery and pressure drop are seen to be decreasing.

4. CONCLUSIONS

The effects of buoyancy on forced convection have been studied for an in-line tube bundle with pitch to diameter ratio of 1.5 and 2.0, $Ri = -1.0, -0.5, 0.0, +0.5, +1.0$. Reynolds numbers of 50, 100 and 150 are considered for the study. With an increase in *Ri*, the flow and heat transfer parameters behave differently. Over the first row of cylinders, the average Nusselt number is found to increase with Richardson number, whereas over the rest of the rows the change is only marginal. The average friction coefficient is found to increase with *Ri* for all the rows of cylinders. Pressure recovery is higher at higher *Ri* and the pressure drop is found to increase with a decrease in *Ri*.

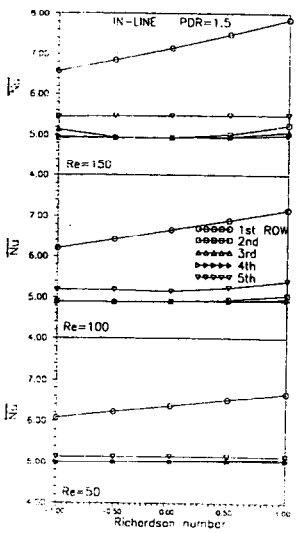

(a) In-line tube bank: PDR=1.5

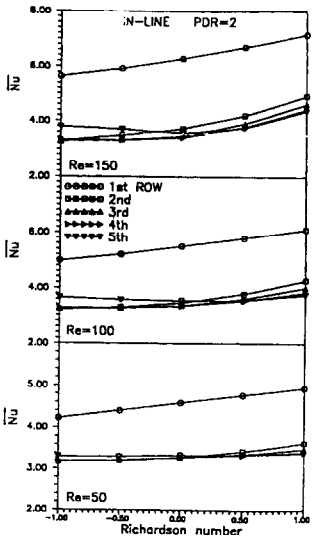

(b) In-line tube bank: PDR=2.0

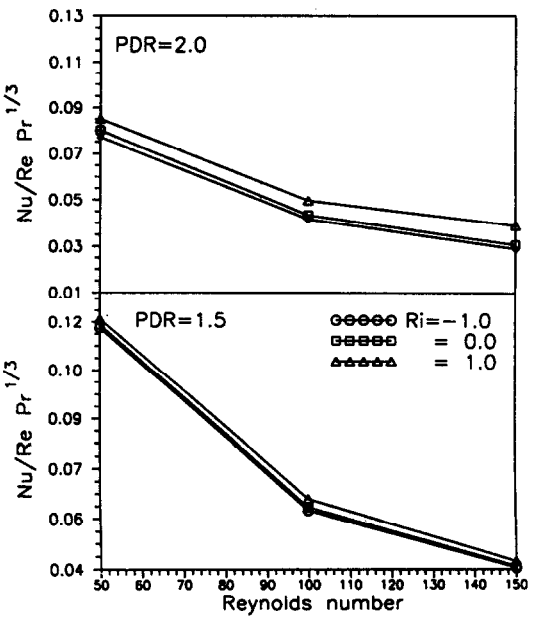

Fig. 5. (a) Variation of average Nusselt numbers. PDR = 1.5. (b) Variation of average Nusselt numbers. PDR = 2.0. (c) Effect of PDR, Reynolds number and *Ri* on average Nusselt numbers.

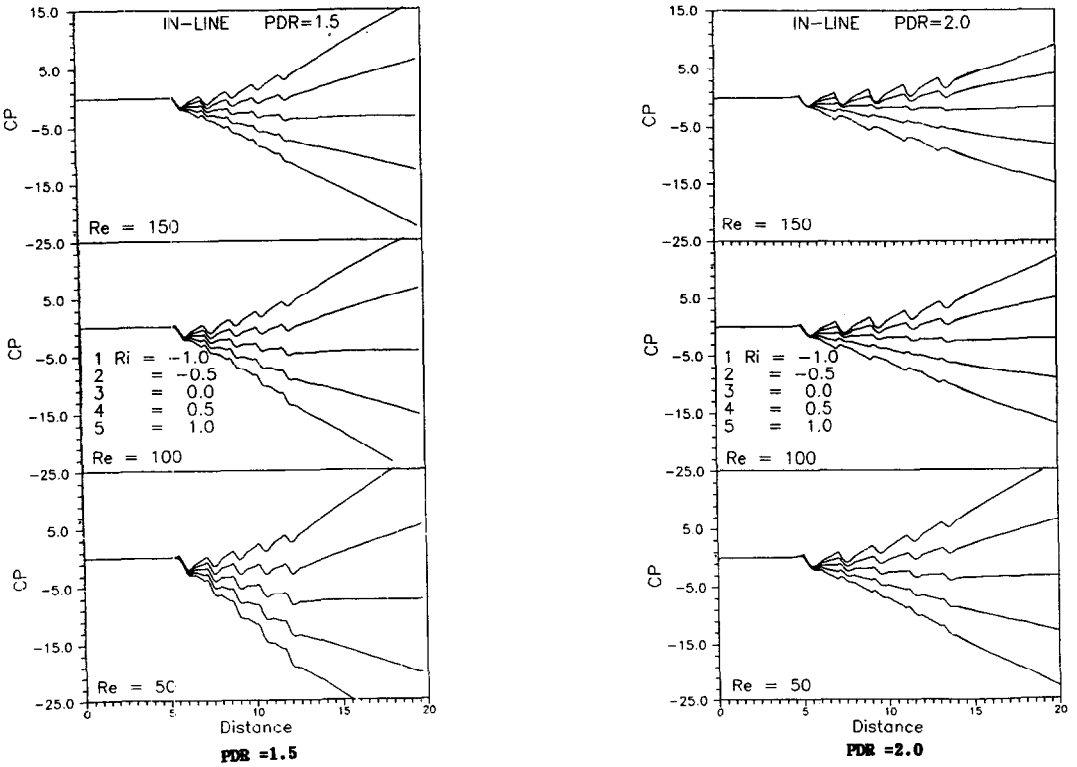

Fig. 6. (a) Pressure distribution around cylinders. PDR = 1.5. (b) Pressure distribution around cylinders. PDR = 2.0.

These results prove that it is essential to consider the buoyancy effects also during the forced convection analysis of flow over tube bundles.

REFERENCES

1. Badr, H. M., A theoretical study of laminar mixed convection from a horizontal cylinder in cross stream. *International Journal of Heat Mass Transfer*, 1983, **26**, 639–653.
2. Badr, H. M., Laminar combined mixed convection from a horizontal cylinder parallel and contra flow regime. *International Journal of Heat Mass Transfer*, 1984, **27**, 15–27.
3. Badr, H. M., On the effect of flow direction on mixed convection from a horizontal cylinder. *International Journal for Numerical Methods in Fluids*, 1985, **5**, 1–12.
4. Krause, J. R. and Tarasuk, J. D., An interferometric study from of mixed convection from a horizontal cylinder. In *Fundamentals of Forced Convection and Mixed Convection* ed. F. A. Kulacki and R. D. Boyd, AMSE, HTD 42, 1985, pp. 171–179.
5. Ho, C. J., Wu, M. S. and Jou, J. B., Analysis of buoyancy aided convection heat transfer from a horizontal cylinder in a vertical duct at low Reynolds number. *Wärme- und Stoffübertragung*, 1990, **25**, 337–343.
6. Keun-shik Chang and Jong-youb Sa, The effect of buoyancy on vortex shedding in the near wake of a circular cylinder. *Journal of Fluid Mechanics*, 1990, **220**, 253–266.
7. Zukauskas, A., Heat transfer from tubes in cross flow. *Advances in Heat Transfer*, 1972, **8**, 93–160.
8. Ishihara, K. and Bell, K., Friction factors for in-line tube banks at low Reynolds numbers. *AIChE Symposium Series*, 1975, **68**, 74–80.
9. Fujii, M., Fujii, R. and Nagata, T., A numerical analysis of laminar flow and heat transfer of air to in-line tube banks. *Numerical Heat Transfer*, 1984, **7**, 89–102.
10. Dhaubhadel, M. N., Reddy, J. N. and Telionis, D. P., Penalty finite element analysis for coupled fluid flow and heat transfer for in-line bundle of cylinders in cross flow. *Journal of Non-linear Mechanics*, 1986, **21**, 361–373.
11. Chang, Y., Beris, A. N. and Michaelides, E. E., A numerical study of heat and momentum transfer for tube bundles in cross flow. *International Method for Numerical Methods in Fluids*, **9**, 1381–1394.
12. Donea, J., Guiliani, S. and Lavel, H., Finite element solution of unsteady Navier–Stokes equations by fractional step method. *Computational Methods in Applied Mechanics and Engineering*, 1982, **30**, 53–73.
13. Ramaswamy, B., Jue, T. C. and Akin, J. F., Semi-implicit and xxplicit finite element schemes for coupled fluid/thermal problems. *International Methods for Numerical Methods in Engineering*, 1992, **34**, 675–696.
14. Segerlind, L. J., *Applied Finite Element Analysis*. John Wiley, New York, USA, 1984.
15. Eckert, E. R. G. and Soehngen, E., Distribution of heat transfer coefficients around circular cylinder in cross flow at Reynolds numbers 20 to 500. *Transactions of ASME* 1952, **74**, 343–347.
16. Tritton, D. J., Experiments on flow past a circular cylinder at low Reynolds. *Journal of Fluid Mechanics*, 1959, **6**, 547–568.
17. Jordon, S. K. and Fromm, J. E., Oscillating drag, lift and torque on a circular cylinder in a uniform flow. *Physics of Fluids*, 1972, **15**, 371–376.
18. Jain, P. C. and Goel, B. S., A numerical study of unsteady laminar forced convection from a circular cylinder. *Transaction of ASME, Journal of Heat Transfer*, 1976, **98**, 303–308.